η-meson production in the resonance-energy region

V. Shklyar,[*] H. Lenske, and U. Mosel

Institut für Theoretische Physik, Universität Giessen, D-35392 Giessen, Germany

We perform an updated coupled-channel analysis of η-meson production including all recent photoproduction data on the proton. The dip observed in the differential cross sections at c.m. energies $W = 1.68$ GeV is explained by destructive interference between the $S_{11}(1535)$ and $S_{11}(1560)$ states. The effect from $P_{11}(1710)$ is found to be small but still important to reproduce the correct shape of the differential cross section. For the $\pi^- N \rightarrow \eta N$ scattering we suggest a reaction mechanism in terms of the $S_{11}(1535)$, $S_{11}(1560)$, and $P_{11}(1710)$ states. Our conclusion on the importance of the $S_{11}(1535)$, $S_{11}(1560)$, and $P_{11}(1710)$ resonances in the η-production reactions is in line with our previous results. No strong indication for a narrow state with a width of 15 MeV and the mass of 1680 MeV is found in the analysis. ηN scattering length is extracted and discussed.

I. INTRODUCTION

The discovery of nucleon resonances in the first pion-nucleon scattering experiments provided first indications for a complicated intrinsic structure of the nucleon. Along with establishing the quark picture of hadrons and developments of the constituent quark models, the interest in the study of the nucleon excitation spectra was renewed. The major question was the number of excited states and their properties. This problem was attacked both experimentally and theoretically. On the theory side constituent quark (CQM) models, lattice QCD and Dyson-Schwinger approaches have been developed to describe and predict the nucleon resonance spectra (see, e.g., [1] for a review). The main problem remains, however, a serious disagreement between the theoretical calculations and the experimentally observed baryon spectra. This concerns both the number and the properties of excited states.

On the experimental side pion-induced reactions have been studied to establish resonance spectra. However, due to difficulties in detecting neutral particles most experiments were limited to pion-nucleon elastic scattering with charged particles in the final state. Being the lightest nonstrange particle next to the pion the η meson also becomes an interesting probe to study nucleon excitations. A few experiments have been made in the past to investigate η production. The first near-threshold measurements [2–4] demonstrated that the reaction proceeds through a strong S-wave resonance excitation which was later identified with $S_{11}(1535)$. An extensive study of the $\pi^- p \rightarrow \eta n$ reaction above $W > 1.7$ GeV has been made in [5,6]. Both differential cross section and asymmetry data have been obtained. However, due to possible problems with the energy-momentum calibration [7] the use of these data might lead to wrong conclusions on the reaction mechanism. Note that these problems are present not only in the η measurements [5,6] but also in the charge-exchange data obtained in the same experiment.

Presently the development of the high-duty electron facilities (ELSA, JLAB, MAMI, SPring) offers new possibilities to study the η photoproduction both on the proton (ηp) and on the neutron (ηn). The first measurement of the η photoproduction on the neutron reported an indication for a resonance-like structure in the reaction cross section at $W = 1.68$ GeV [8,9]. Independent experimental studies [10,11] confirmed the existence of this effect in the γn reaction. This phenomenon was predicted in [12] as a signal from a narrow state—a possible nonstrange partner of the pentaquark [13]. Another explanation has been suggested in [14] where the observed effect was described by the contributions from the $S_{11}(1650)$ or $P_{11}(1710)$ states. Due to the lack of knowledge of the $S_{11}(1650)$ and $P_{11}(1710)$ resonance couplings to γn a clean separation of the relative contributions from these states is difficult. The general conclusion made in [14] is that both states might be good candidates to explain the observed structure.

By fitting to the ηn cross sections and beam asymmetry the Bonn-Gatchina group provided an explanation [15] for the second peak in terms of the $S_{11}(1650)$ state. Another contribution to the field has been made by the authors of [16]. There the peak in the σ_p/σ_n cross section ratio was explained by a cusp effect from the $K\Sigma$ and $K\Lambda$ rescattering channel. All these studies have been done assuming scattering on a quasifree nucleon. At the same time a realistic analysis of meson photoproduction on the quasifree neutron should include the nucleon-nucleon and meson-nucleon correlations (FSI-effect) which were shown to be very important [17] and take into account corresponding experimental cuts applied by the extraction of the quasifree neutron data from γD scattering. The later issue might be crucial for the unambiguous identification of the narrow resonance contribution as discussed in [18].

If it is granted that the signal observed in the γn scattering [8–11] is due to the narrow (exotic) state one may expect to observe a similar effect in other η-production reactions at the same energies, e.g., in γ-proton scattering. The experimental investigations of the η production on the proton made by the CLAS, GRAAL, and CB-ELSA/TAPS collaborations [19–22] have found an indication of the dip structure around $W = 1.68$ GeV in the differential cross section but not a resonance-like structure. This effect was also accompanied by the change in the angular distribution of the differential cross section. However, despite of extensive theoretical studies

————
[*]shklyar@theo.physik.uni-giessen.de

of the η production the reaction mechanism is still under discussion [21,23–34].

Recently the η photoproduction on the proton was measured with high-precision by the Crystal Ball collaboration at MAMI [35]. These high-resolution data provides a new step forward in understanding the reaction dynamics and in the search for a signal from the 'weak' resonance states. The main result reported in [35] is a very clean signal of a dip structure around $W = 1.68$ GeV. It is interesting to note that the old measurements of the $\pi N \to \eta N$ reaction [3] also give an indication for the second structure in the differential cross section at $W = 1.7$ GeV. This raises a question whether the dip reported in the ηp reaction, the resonance-like signal observed in ηn and the possible structure in the $\pi N \to \eta N$ cross section are originating from the same degrees of freedom or not. The second question is whether one of these phenomena can be attributed to the signal from a narrow (exotic) resonance state as discussed in [12,36,37].

In our previous coupled-channel PWA study [14] we proposed an explanation of the possible dip in the η-proton cross section in terms of the destructive interference of the $S_{11}(1535)$ and $S_{11}(1650)$ states. The result was based on the ηp photoproduction data taken before 2006 [19,38]. The aim of the present study is to extend our previous coupled-channel analysis of the $\gamma p \to \eta p$ reaction by including the data from the high-precision measurements [35]. The main question is whether the ηp reaction dynamics can be understood in terms of the established resonance states. We emphasize that for reliable identification of the resonance contributions the calculations should maintain unitarity. Another complication comes from the fact that the most contributions to the resonance self-energy (total decay width) is driven by its hadronic couplings. Therefore the analysis of the photoproduction data requires the knowledge of the hadronic transition amplitudes. Hence the simultaneous analysis of all open channels (both hadronic and electromagnetic) is inevitable for the identification of the resonances and extraction of their properties. In the present study we concentrate on the combined description of the $(\gamma/\pi)p \to \eta p$ scattering taking also the $(\gamma/\pi) \to \pi N, 2\pi N,$ $\omega N, K\Lambda$ channels into account. The results on the ηn reaction will be reported elsewhere.

First, we corroborate our previous findings [14,39,40] where the important contributions from the $S_{11}(1535)$, $S_{11}(1650)$, and $P_{11}(1710)$ resonances to the $\pi N \to \eta N$ reaction have been found. The major effect comes from the S_{11} and P_{11} partial waves. The interference between the $S_{11}(1535)$ and $S_{11}(1650)$ states produces a dip in the S_{11} amplitude. The P_{11} amplitude is influenced by the contributions from the $P_{11}(1710)$ state. The interference between the S_{11} and P_{11} partial waves leads to the forward peak in the differential cross section around $W = 1.7$ GeV. We stress that the interference between two nearby states also includes rescattering and coupled-channel effects which are hard to simulate by the simple sum of two Breit-Wigner forms.

We also confirm our previous finding that the interference between $S_{11}(1535)$ and $S_{11}(1650)$ is responsible for the dip seen in the ηp data. The effect from the ωN threshold is found to be relatively small which is also in line with the conclusion of [14]. Opposite to [27] we do not find any strong indications

for a narrow state in the Crystal Ball/Taps data around $W = 1.68$ GeV. We have also checked our results for the ηp reaction above $W = 2$ GeV where a number of new experimental data are available. Note that we do not use Reggezied t-channel exchange but include all t-channel contributions consistently into our unitarization procedure. Because of the normalization problem [41,42] between the CLAS [43] and the CB-ELSA [20] data sets, the simultaneous description of these data is not possible. Above $W = 2$ GeV our calculations are found to be in closer agreement with the CLAS measurements [43]. The CB-ELSA data [20] demonstrates a step rise around $W = 1.925$ GeV for the scattering angles $\cos\theta = 0.85, \ldots, 0.95$. It is not clear whether this phenomenon could be related to a threshold effect [e.g., ϕN, $a_0(980)N$, $f_0(980)$, or $\eta' N$] or attributed to other reaction mechanisms.

We conclude that further progress in understanding of the η-meson production dynamics would be hardly possible without new measurements of the $\pi N \to \eta N$ reaction.

II. DATABASE

Here we present a short overview of the experimental database relevant for the present calculations. The details on the $K\Lambda$, $K\Sigma$, ωN channels will be given elsewhere.

$\pi N \to \eta N$: The thorough overview of the $\pi N \to \eta N$ experimental data (except the recently published Crystal Ball measurements [44]), is given in [7]. As already mentioned in the Introduction only a few measurements of the η production have been made with pion beams: except for [45] where the η meson was produced in $\pi^+ D$ collisions, all the data have been taken from the $\pi^- p$ scattering [2–6,44,46,47]. Unfortunately due to numerous problems with the experimental data from [5,6] (see discussion in [7] and references therein) the use of these measurements in the analysis might lead to wrong conclusions for the reaction mechanism. Therefore, opposite to [48] we do not include these data in the analysis. Another measurement available above $W = 1.65$ GeV is the data from Richards et al. [3]. In the first resonance energy region this cross section tends to be lower than results from other experiments. Since the old measurements quote only statistical uncertainties the reason for these differences is unclear. In their study the authors of [49] added systematical errors to all differential cross sections. We do not follow this procedure and include only quoted uncertainties in the analysis.

$\gamma p \to \eta p$: a number of experimental studies have been performed in the resonance energy region [19–22,35,38,43, 50–55]. Most of these measurement are differential cross sections. The target asymmetry has been studied in [54]. It has been observed that close to the ηN production threshold the asymmetry changes the sign at moderate scattering angles. The previous calculations of the Giessen model [14,39] and the Mainz group [56] could not explain this feature. The description of this data would require an unexpected phase shift between the S_{11} and D_{13} resonances as noted in [56]. One may hope that the upcoming new measurements of the target asymmetry at the ELSA facility will solve this puzzle [57].

For the beam asymmetry we use the recent data from the GRAAL [22] and CB-ELSA/TAPS [53] collaborations

which cover the energy region up to $W = 1.91$ GeV. For the differential cross section we use the recent high-quality Crystal Ball data [35]. Above $W = 1.89$ GeV our calculations are constrained by the amalgamated data set from experiments [20,21,38,43]. Since the experimental uncertainties of the data [20,21,38,43] are much larger than those in [35] we reduce them by factor of 2.

In the $(\pi/\gamma)N \to \pi N$ channels our calculations are constrained by the single-energy solutions from the GWU (formerly SAID) analysis [58–60]. For the $\pi N \to 2\pi N$ transitions we follow the procedure described in [25,39,40,61]. We continue to parametrize the $2\pi N$ channel in terms of the effective ζN state, where ζ is an isovector scalar meson of two pion mass: $m_\zeta = 2m_\pi$. The final ζN state is only allowed to couple to nucleon resonances. Therefore the decay $N^* \to \zeta N$ stands for the sum of transitions $N^* \to \Delta\pi, \sigma N, \rho N$, etc. This procedure allows for the good description of the $\pi N \to 2\pi N$ partial wave cross sections extracted in [62]. However of case of the $\gamma p \to 2\pi N$ the same agreement cannot be expected. This is because of the enhanced role of the background contributions (due to, e.g., the contact $\gamma\rho N N$ interaction in the $\gamma N \to \rho N$ transitions). After fixing the database a χ^2 minimization is performed to fix the model parameters.

III. GIESSEN MODEL

Here we briefly outline the main ingredients of the model. More details can be found in [25,39,40,61,63,64]. The Bethe-Salpeter equation is solved in the K-matrix approximation to obtain multichannel scattering T matrix:

$$T(\sqrt{s}, p, p') = K(\sqrt{s}, p, p') + \int \frac{d^4q}{(2\pi)^4} K(\sqrt{s}, p, q) G_{BS}$$
$$\times (\sqrt{s}, q) T(\sqrt{s}, q, p'), \qquad (1)$$

where p (k) and p' (k') are the incoming and outgoing baryon (meson) four-momenta, $T(\sqrt{s}, p, p')$ is a coupled-channel scattering amplitude, G_{BS} is a meson-nucleon propagator and $K(\sqrt{s}, p, p')$ is an interaction kernel. The quantities $T(\sqrt{s}, p, p')$, G_{BS}, and $K(\sqrt{s}, p, p')$ are in fact multidimensional matrices where the elements of the matrix stand for the different scattering reactions.

To solve the coupled-channel scattering problem with a large number of inelastic channels, we apply the so-called K-matrix approximation by neglecting the real part of the BSE propagator G_{BS}. After the integration over the relative energy, Eq. (1) reduces to

$$T_{fi}^{\lambda_f \lambda_i} = K_{fi}^{\lambda_f \lambda_i} + i \int d\Omega_n \sum_n \sum_{\lambda_n} T_{fn}^{\lambda_f \lambda_n} K_{ni}^{\lambda_n \lambda_i}, \qquad (2)$$

where T_{fi} is a scattering matrix and $\lambda_i(\lambda_f)$ stands for the quantum numbers of initial(final) states $f, i, n = \gamma N$, πN, $2\pi N$, ηN, ωN, $K\Lambda$, $K\Sigma$. Using the partial-wave decomposition of T, K in terms of Wigner d functions the angular integration can be easily carried out and the equation is further simplified to the algebraic form

$$T_{fi}^{J\pm,I} = \left[\frac{K^{J\pm,I}}{1 - iK^{J\pm,I}} \right]_{fi}. \qquad (3)$$

The validity of this approximation was demonstrated by Pearce and Jennings in [65] by studying different approximations to the BSE for πN scattering. Considering different BSE propagators they concluded that an important feature of the reduced intermediate two particle propagator is the on-shell part of G_{BS}. It has been argued that there is no much difference between physical parameters obtained using the K-matrix approximation and other schemes. It has also been shown in [66,67] that for πN and $\bar{K}N$ scattering the main effect from the off-shell part is a renormalization of the couplings and the masses.

Due to the smallness of the electromagnetic coupling the dominant contributions to the self energy stem from the hadronic part. Therefore we treat the photoproduction reactions perturbatively. This is equivalent to neglecting γN in the sum over intermediate states n in Eq. (2). Thus, for a photoproduction process Eq. (3) can be rewritten as follows [25,40]:

$$T_{f\gamma}^{J\pm,I} = K_{f\gamma}^{J\pm,I} + i \sum_n T_{fn}^{J\pm,I} K_{n\gamma}^{J\pm,I}, \qquad (4)$$

where the summation in Eq. (4) is done over all hadronic intermediate states. Here the matrix $T_{fn}^{J\pm,I}$ stems only from the hadronic transitions: indices f and n run over πN, $2\pi N$, ηN, $K\Lambda$, $K\Sigma$, ωN channels. The sum in Eq. (4) reflects the importance of the hadronic part of the transition amplitude in the description of photoproduction reactions. In other words, the amplitudes for the $\pi N \to \pi N$, ηN, ωN, etc. transitions should always be included in the calculation of the photoproduction amplitudes.

A. Interaction kernel and resonance parameters

Here we present the main ingredients of the interaction kernel to the BSE Eq. (1) relevant for η production. More details on other reactions can be found in [25,39,40,61,63,68]. The interaction potential (K matrix) of the BSE is built up as a sum of s-, u-, and t-channel contributions corresponding to the tree level Feynman diagrams shown in Fig. 1. In the isospin $I = \frac{1}{2}$ channel we checked for the contributions from the $S_{11}(1535)$, $S_{11}(1650)$, $P_{11}(1440)$, $P_{11}(1710)$, $P_{13}(1720)$, $P_{13}(1900)$, $D_{13}(1520)$ $D_{13}(1900)$, $D_{15}(1675)$, $F_{15}(1680)$, $F_{15}(2000)$ resonances. The resonance and background contributions are consistently generated from the same effective interaction. The Lagrangian densities are given in [25,39,40,61,63,68] and respect the chiral symmetry in low-energy regime. The properties of the t-channel mesons important for η production are given in Table I. Using the interaction Lagrangians and values of the corresponding meson decay widths taken from the PDG [69] the following coupling constants are obtained:

$$g_{a_0\eta\pi} = -2.100\,, \quad g_{\omega\eta\gamma} = -0.27\,,$$
$$g_{\rho\eta\gamma} = -0.64\,, \quad g_{\phi\eta\gamma} = -0.385\,. \qquad (5)$$

All other coupling constants were allowed to be varied during the fit. The obtained values are given in Table II. For the $\eta N N$ interaction we use pseudoscalar coupling, which has been also utilized in our previous studies [14,25,39,40,61]. The derived $g_{\eta N N}$ constant is found to be small which is in
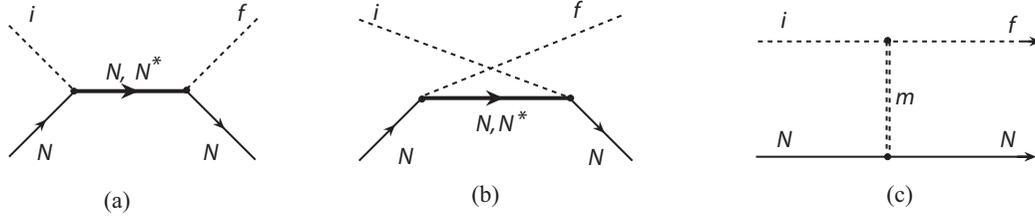
FIG. 1. s-, u-, and t-channel contributions to the interaction potential. i and f stand for the initial and final γN, πN, $2\pi N$, ηN, ωN, $K\Lambda$, $K\Sigma$ states. m denotes intermediate t-channel meson.

line with our previous results [14,40]. To check the dependence of our results on the choice of the ηNN interaction we have also performed calculations with the pseudovector coupling. However also in the latter case only a small $g_{\eta NN}$ coupling constant has been found.

Since the PDG gives only the upper limit for the decay branching ratio $R(\rho \to \pi\eta) < 6 \times 10^{-3}$ we allowed this constant to be varied during fit. However due to lack of experimental constraints this coupling cannot be fully fixed in the present calculation. We find a small overall contribution from the t-channel ρ-meson exchange to the $\pi^- p \to \eta n$ reaction. The $g_{\phi NN}$ coupling is calculated from $g_{\omega NN}$ using the relation

$$\frac{g_{\phi NN}}{g_{\omega NN}} = -\tan \Delta\theta_{\phi/\omega},$$

where $\Delta\theta_{\phi/\omega}$ is a deviation from the ideal ϕ-ω mixing angle. Taking $\Delta\theta_{\phi/\omega} = 3.7°$ from [69] one gets for the ratio $g_{\phi NN}/g_{\omega NN} \approx -1/15$. Using this value a very small contribution from the t- channel ϕ-meson exchange to the η photoproduction has been found.

To take into account the finite size of mesons and baryons each vertex is dressed by a corresponding form factor:

$$F_p(q^2, m^2) = \frac{\Lambda^4}{\Lambda^4 + (q^2 - m^2)^2}, \qquad (6)$$

where q is a c.m. four-momentum of an intermediate particle and Λ is a cutoff parameter. The cutoffs Λ in Eq. (6) are treated as free parameters being varied during the calculation. However, we keep the same cutoffs in all channels for a given resonance spin J : $\Lambda^J_{\pi N} = \Lambda^J_{\pi\pi N} = \Lambda^J_{\eta N} = \ldots$, etc., ($J = \frac{1}{2}, \frac{3}{2}, \frac{5}{2}$). This significantly reduces the number of free parameters; i.e., for all spin-$\frac{5}{2}$ resonances there is only one cutoff $\Lambda = \Lambda_{\frac{5}{2}}$ for all decay channels. However for the photoproduction reactions we use different cutoffs at the s- and u-channel electromagnetic vertices. All values are given

in Table III. Except for the spin-$\frac{3}{2}$ states, the s- and u-channel cutoffs almost coincide.

The use of vertex form factors requires special care for maintaining the current conservation when the Born contributions to photoproduction reactions are considered. Since the resonance and intermediate meson vertices are constructed from gauge invariant Lagrangians they can be independently multiplied by the corresponding form factors. For the nucleon contributions to meson photoproduction we apply the suggestion of Davidson and Workman [70] and use the crossing symmetric common form factor:

$$\tilde{F}(s, u, t) = F(s) + F(u) + F(t) - F(s)F(u) - F(s)F(t) \\ - F(u)F(t) + F(s)F(u)F(t). \qquad (7)$$

The extracted resonance parameters given in Table IV are very close to the values deduced in our previous calculations [14,68] which indicates the stability of the obtained solution. However some values changed upon inclusion of the new MAMI data [35]. The total width of $S_{11}(1650)$ tends to be larger than that deduced in our previous calculations [68]. The helicity amplitude is also modified but still is in good agreement with the parameter range provided by PDG [69]. The opposite effect is found for the $P_{11}(1710)$ state where the total width is reduced once the data of [35] are included. The remaining resonance parameters are only slightly modified as compared to our previous results.

The mass and width of the Roper resonance is found to be larger than deduced in other analyses [69]. However the authors of [71] give 490 ± 120 MeV for the total width. The large decay width 545 ± 170 MeV has also been deduced by Cutkosky and Wang [72]. Note that properties of this state are strongly influenced by its decay into the $2\pi N$ final state. Arndt $et\ al.$ [73] found a second pole structure for the Roper resonance which might be attributed to the coupling to the $\pi\Delta$ subchannel. Since we use a simplified prescription for the $2\pi N$ reaction this effect cannot be properly described in the present calculations.

The recent GWU(SAID) study of the πN data shows no evidence for the $P_{11}(1710)$ resonance. An indirect indication for the existence of this state can be concluded from the

TABLE I. Properties of mesons which give contributions to the ηN final state via the t-channel exchange. The notation (γ, η) means $\gamma N \to \eta N$, etc.

	mass [GeV]	J^P	I	final state
ω	0.783	1^-	0	(γ, η)
ρ	0.769	1^-	1	$(\pi, \eta)(\gamma, \eta)$
a_0	0.983	0^+	1	(π, η)
ϕ	1.02	1^-	0	(γ, η)

TABLE II. Nucleon and t-channel couplings obtained in the present study.

$g_{\pi NN}$	12.85	$g_{\rho\eta\pi}$	0.133	$g_{\rho NN}$	4.98	κ_ρ	2.18
$g_{\eta NN}$	0.31	$g_{a_0 NN}$	-44.37	$g_{\omega NN}$	7.23	κ_ω	-1.50

TABLE III. Cutoff values for the form factors. The lower index denotes an intermediate particle, i.e., N: nucleon, $\frac{1}{2}$: spin-$\frac{1}{2}$ resonance, $\frac{3}{2}$: spin-$\frac{3}{2}$, $\frac{5}{2}$: spin-$\frac{5}{2}$ resonance, t: t-channel meson. The upper index $h(\gamma)$ denotes whether the value is applied to a hadronic or electromagnetic vertex. The cutoff values used at electromagnetic u-channel vertices are given in brackets.

Λ_N [GeV]	$\Lambda_{\frac{1}{2}}^h$ [GeV]	$\Lambda_{\frac{3}{2}}^h$ [GeV]	$\Lambda_{\frac{5}{2}}^h$ [GeV]	$\Lambda_{\frac{1}{2}}^\gamma$ [GeV]	$\Lambda_{\frac{3}{2}}^\gamma$ [GeV]	$\Lambda_{\frac{5}{2}}^\gamma$ [GeV]	$\Lambda_t^{h,\gamma}$ [GeV]
0.952	3.0	0.97	1.13	1.69 (1.69)	4.20 (2.9)	1.17 (1.25)	0.7

analysis of the πN inelasticity and $2\pi N$ cross section in the P_{11} partial wave, see discussion in Sec. IV. We find a small coupling of this resonance to the πN final state. Since a clear signal from this state is not seen in the recent GWU solution, the determination of the total width turns out to be difficult. In our calculations we assume that this resonance has a large decay branching ratio to the ηN. However the quality of the $\pi^- p \to \eta n$ data does not allow for an unambiguous determination of the properties of this state.

The mass and width of the $D_{13}(1520)$ is more close to the values obtained by Arndt *et al.* [74]: 1516 ± 10 MeV and 106 ± 4 MeV, respectively. It is interesting to note that the mass of this resonance deduced from the pion photoproduction tends to be 10 MeV lower that the values derived from the pion-induced reactions [69]. The second $D_{13}(1900)$ has a very large decay width. We associate this state with $D_{13}(2080)$ as suggested by the Particle Data Group (PDG). This resonance is rated with two stars and its existence

TABLE IV. Resonance parameters extracted in the present study. The uncertainties are given in brackets. Helicity decay amplitudes are given in $10^{-3}\text{GeV}^{-\frac{1}{2}}$. First line: present study; second line: [68], third line: [69]. (–): the validity range is not given.

N^*	mass (MeV)	Γ_{tot}(MeV)	$R_{\pi N}$	$R_{2\pi N}$	$R_{\eta N}$	$R_{\omega N}$	$A_{\frac{1}{2}}^p$	$A_{\frac{3}{2}}^p$
$S_{11}(1535)$	1526(2)	131(12)	35(3)	8(2)	58(4)	–	91(4)	–
	1526	136	34.4	9.5	56.1	–	92	–
	1536(10)	150(25)	45(10)	5(5)	42(10)	–	90(30)	–
$S_{11}(1650)$	1665(2)	147(14)	74(3)	23(2)	1(2)	–	63(6)	–
	1664	131	72.4	23.1	1.4	–	57	–
	1657(13)	150(30)	70(20)	15(5)	10(5)	–	53(16)	–
$P_{11}(1440)$	1515(15)	605(90)	56(2)	44(2)	–	–	−85(3)	–
	1517	608	56.0	44.0	–	–	−84	–
	1445(25)	300(150)	65(10)	35(5)	–	–	−60(4)	–
$P_{11}(1710)$	1737(17)	368(120)	2(2)	49(3)	45(4)	3(2)	−50(1)	–
	1723	408	1.7	49.8	43.0	0.2	−50	–
	1710(30)	150(100)	13(7)	65(25)	20(10)	13(2)	24(10)	–
$P_{13}(1720)$	1700(10)	152(2)	17(2)	79(2)	0(1)	–	−65(2)	35(2)
	1700	152	17.1	78.7	0.2	–	−65	35
	1725(24)	225(125)	11(3)	>70	4(1)	–	50(60)	−19(20)
$P_{13}(1900)$	1998(3)	359(10)	25(1)	61(2)	2(2)	10(3)	−8(1)	0(1)
	1998	404	22.2	59.4	2.5	14.9	−8	0
	1900(-)	250(-)	10(-)	–	12(−)	39(-)	26(15)	−65(30)
$D_{13}(1520)$	1505(4)	100(2)	57(2)	44(2)	0(1)	–	−15(1)	146(1)
	1505	100	56.6	43.4	1.2	–	−13	145
	1520(5)	112(12)	60(5)	25(5)	2.3×10^{-3}	–	−24(8)	150(15)
$D_{13}(1875)$	1934(10)	857(100)	11(1)	69(2)	0(1)	20(5)	11(1)	26(1)
	1934	859	10.5	68.7	0.5	20.1	11	26
	1875(45)	220(100)	12(10)	70(20)	3.5(3.5)	21(7)	18(10)	−9(5)
$D_{15}(1675)$	1666(2)	148(1)	41(1)	58(1)	0(1)	–	9(1)	21(1)
	1666	148	41.1	58.5	0.3	–	9	20
	1675(5)	150(15)	40(5)	55(5)	0(1)	–	19(8)	15(9)
$F_{15}(1680)$	1676(2)	115(1)	68(1)	32(1)	0(1)	–	3(1)	116(1)
	1676	115	68.3	31.6	0.0	–	3	115
	1685(5)	130(10)	67(3)	35(5)	0(1)	–	−15(6)	132(13)
$F_{15}(2000)$	1946(4)	198(2)	10(1)	87(1)	2(2)	1(1)	11(1)	25(1)
	1946	198	9.9	87.2	2.0	0.4	10	25
	2050(100)	350(200)	15(7)	–	–	–	35(15)	50(14)

is still under discussion. In our updated coupled-channel calculation of the ω production [68] a large ωN and $2\pi N$ decay branching ratios have been obtained.

The properties of other resonances are very close to the values given by the PDG. Except for $S_1(1535)$ and $P_{11}(1710)$ we find only small resonance couplings to ηN which is in accordance with our previous conclusions. One needs to stress that the smallness of the resonance coupling does not necessarily mean that the contribution from the state is negligible. The $S_{11}(1650)$ state produces for example a sizable effect in the η production due to overlapping with $S_{11}(1535)$. Another example is the effect from the $D_{13}(1520)$ state in η photoproduction on the proton. Here the smallness of the ηN branching ratio is compensated by the strong electromagnetic coupling of this resonance. Therefore the effect from this state could be seen in the E_{2-} and M_{2-} multipoles, see Sec. IV E. However in most cases the resonance contributions with small branching ratios to the η are hard to resolve unambiguously.

B. Pole parameters

It is interesting to compare the poles positions and elastic residues with the results from other studies, see Table V. The calculated pole masses are very close to the values obtained in other analyses, see [69]. The agreement between imaginary parts and elastics residues is also good, though some differences exist between the present values and the results from other groups.

For the $S_{11}(1535)$ state we obtain a smaller elastic residue (for definition of $|R|$ see [69]) $|R| = 15$ MeV which is almost identical to the result of the GWU group $|R| = 16$ MeV [59].

Both values seem to be out of the range given in PDG [69] 50 ± 20 MeV. It is interesting to note that the elastic residue from [59] is included into the estimation made in [69] but still does not fit to the provided range. The value $\Gamma_{\text{pole}} = 89$ MeV for the $S_{11}(1650)$ state is also comparable with the result from [59]: $\Gamma_{\text{pole}} = 80$ MeV which are again less than the lower bound given in [69].

Though the derived pole mass of $P_{11}(1440)$ is very close to the values deduced in other calculations we obtain a significantly larger pole width. As a result the elastic pole residue turns out to be also large $|R| = 126$ MeV. We note, that the extraction of the properties of $P_{11}(1440)$ in the complex energy plane might require a proper treatment of the $P_{11}(1440) \rightarrow \pi \Delta(1232) \rightarrow 2\pi N$ isobar decay channel where the overlap of the self-energies of the $P_{11}(1440)$ and $\Delta(1232)$ states might be important for the determination of the properties of $P_{11}(1440)$. This question will be addressed in [75].

As we already mentioned the results for $P_{11}(1710)$ are controversial. We find 159 MeV for the pole width. Somewhat greater value of 189 MeV has been obtained in [76,77]. The recent issue of the PDG [69] summarizes results for the pole parameters taken from four different analyses. Whereas the calculations [78,79] give 200 MeV for the pole width, Cutkosky obtains a significantly lower value $\Gamma = 80$ MeV [80,81]. This results in a large spread of the resonance width given by the PDG, see Table V. The elastic residue is found to be small which is in accordance with the small decay branching ratio to πN. The similar conclusion has also been drawn in [76].

Investigation of the P_{13}-wave inelasticity [59] shows that the $P_{13}(1720)$ state could have a strong decay flux into the $3\pi N$ channel [62]. Therefore the calculation of its pole width

TABLE V. Pole positions and elastic pole residues. First line: present study, second line: values from PDG [69].

	Re z_0(GeV)	-2Im z_0(MeV)	$|R|$(MeV)	θ^0
$S_{11}(1535)$	1.49	100	15	-51
	1.49–1.53	90–250	30...70	$-1...-30$
$S_{11}(1650)$	1.65	89	19	-46
	1.64–1.67	100–170	20–50	$-50...-80$
$P_{11}(1440)$	1.386	277	126	-60
	1.35–1.38	160–220	40–52	$-75...-100$
$P_{11}(1710)$	1.67	159	11	9
	1.67–1.77	80–380	2–15	$-160...+190$
$P_{13}(1720)$	1.67	118	12	-45
	1.66–1.69	150–400	7–23	$-90...-160$
$P_{13}(1900)$	1.91	173	10	-64
	1.870–1.93	140–300	1–5	$45...-25$
$D_{13}(1520)$	1.492	94	27	-35
	1.505–1.515	105–120	32–38	$-5...-15$
$D_{13}(1875)$	1.81	98	3	-76
	1.8–1.95	150–250	2–10	$20...180$
$D_{15}(1675)$	1.64	108	20	-49
	1.655–1.665	125–150	22–32	$-21...40$
$D_{15}(1680)$	1.66	98	33	-32
	1.665–1.68	110–135	35–45	$0...-30$
$F_{15}(2000)$	1.90	123	11	-6
	1.92–2.15	380–580	20–115	$-60...-140$

might be affected by deficiencies in description of this channel. PDG estimations are based on several studies where $\Gamma_{\text{pole}} = 120 \pm 40$ by Cutkosky [81] is the lower limit. The upper bound $\Gamma_{\text{pole}} = 450 \pm 100$ MeV is given by the recent Bonn-Gatchina analysis [78]. Neither of these calculations includes the $3\pi N$ channel explicitly.

The situation with the second $P_{13}(1900)$ state is even more complicated. This resonance is rated by two stars in PDG and supposed to be rather broad. The latest GWU analysis [59] does not find any indication for this state. The present information about the pole parameters in PDG is based solely on the result of the Bonn-Gatchina calculations [78] which deduce the pole mass 1900 ± 30 MeV and the pole width 200^{+100}_{-60} MeV. These values are very close to those derived in the present work.

The pole width of the $D_{13}(1520)$ state(94 MeV) turns out to be 10 MeV less than the lower limit given by the PDG [69]. The similar value of $\Gamma_{\text{pole}} = 95$ MeV has also been obtained in the Jülich model [82]. Some analyses find additional poles associated with the $D_{13}(1700)$ and $D_{13}(1875)$ states [69]. We do not find any indication for $D_{13}(1700)$. The pole position for the second resonance is close to the results of other calculation [69].

Though the elastic residues for the $D_{15}(1675)$ and $F_{15}(1680)$ states are comparable with the values given by the PDG their pole widths are somewhat lower than those obtained in other studies [69]. We also find an indication for the second state $N(2000)$ with the pole mass of 1900 MeV and the width of 123 MeV, see Table V. This resonance has a small coupling to the πN final state what is in agreement with results from other calculations.

IV. RESULTS AND DISCUSSION

The lack of the experimental data for the pion-induced reactions does not provide enough constraints on the resonance parameters. Also the discrepancy among various measurements (see Sec. II) does not allow for a consistent description of the data in a full kinematical region. While the contribution from the $S_{11}(1535)$ state is well established the reaction dynamics above $W = 1.6$ GeV is still under discussion. One of the early Giessen coupled-channel calculations [14,39,40] found a destructive interference between $S_{11}(1535)$ and $S_{11}(1650)$ states. The second suggestion is a strong contribution from the $P_{11}(1710)$-resonance excitation above $W = 1.68$ GeV. This resonance was established in the early single-channel Karlsruhe-Helsinki and Carnegie Mellon-Berkeley analyses (see PDG [69] and references therein). The independent study of the $\pi N \to (\pi/\eta) N$ reactions by the Zagreb group [83] provides an additional evidence for the existence of $P_{11}(1710)$. The result of [83] confirm the assumption made in [39,40] on the important contribution from this state to the η production. However the recent analysis from the GWU group [59] finds no evidence for this state. The absence of a clear signal in the P_{11} partial wave of the elastic πN scattering does not necessarily mean that this state does not exist. If the coupling to the final πN state is small, the effect from this state might not be seen in πN scattering. The evidence for the signal from the $P_{11}(1710)$ resonance has also been reported from the study
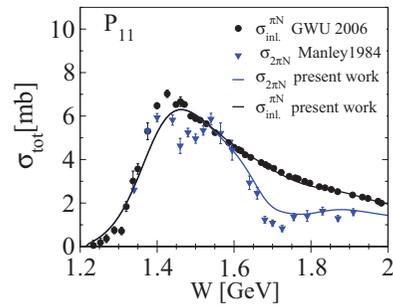
FIG. 2. (Color online) Calculated πN inelasticity and $\pi N \to 2\pi N$ cross section in the P_{11} partial wave in comparison with the results from [59] (GWU 2006) and [62] (Manley 1984).

of the $\pi N \to K\Lambda$ reaction [84]. On the other hand the result of the Bayesian analysis performed by the Gent group [85] demonstrates that $P_{11}(1710)$ is not needed to describe the $K\Lambda$ photoproduction. An opposite conclusion was drawn by the Bonn-Gatchina group which finds decay branching ratio of $23 \pm 7\%$ of this state to $K\Lambda$ [78].

Another indication for this state comes from the analysis of an inelastic flux in the P_{11} partial wave. In Fig. 2 the total inelasticity from the GWU analysis vs. the total 2π cross section extracted in [62] is compared. The difference between the total πN inelasticity and the total $2\pi N$ cross section at $W = 1.7$ GeV in the P_{11} wave can be attributed to the sum of inelastic channels like $3\pi N$, ηN, $\eta\pi N$, etc. We assume here that the observed difference is due to the ηN production channel dominated by the $P_{11}(1710)$ state. As $g_{\pi NN^*(1710)}$ is assumed to be small this raises the question about the magnitude of the $P_{11}(1710)$ contribution in the $\pi N \to \eta N$ reaction. However the situation in η production is different from the πN elastic scattering. Here the contribution from $P_{11}(1710)$ is proportional to the product $g_{\pi NN^*(1710)}g_{\eta NN^*(1710)}$, where $g_{\pi NN^*(1710)}$ is the coupling constant at the $N(1710) \to \eta N$ transition vertex. It follows that the contribution from the $P_{11}(1710)$ can be significant provided that $g_{\eta NN^*(1710)}$ is large enough. The interplay with background and coupled-channel rescattering would further increase this effect.

A. $\pi N \to \eta N$

The results of our calculations are presented in Fig. 3 in comparison with the world data. The first peak at $W = 1.54$ GeV is related to the well established $S_{11}(1535)$ resonance contribution.

Though the effect from the $S_{11}(1650)$ state is hardly visible in the differential cross section this state plays an important role leading to the destructive interference between $S_{11}(1535)$ and $S_{11}(1650)$ as it has been pointed out in our previous calculations [39,40].

The second rise is due to the $P_{11}(1710)$ resonance. This state has a small branching ratio to the πN system but due to the large η coupling this resonance affects the production cross section at $W = 1.7$ GeV. The coupled-channel effects and interference with other partial waves further enlarge the overall contribution from this state.
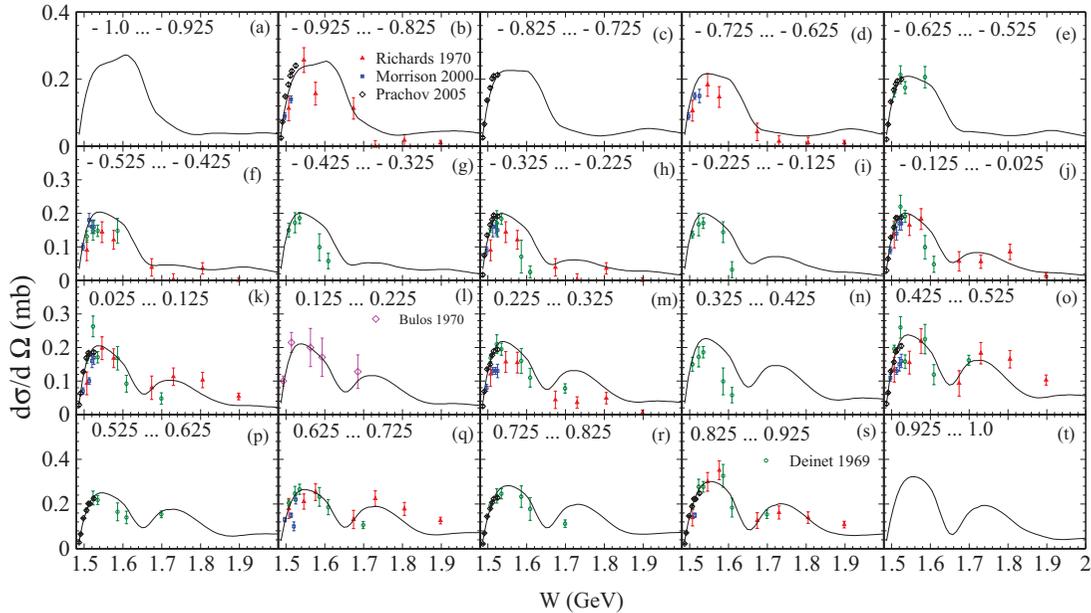
FIG. 3. (Color online) Calculated differential $\pi^- p \to \eta n$ cross section in comparison with the experimental data from: Prakhov 2005 [44], Deinet 1969 [47], Richards 1970 [3], Morrison 2000 [86].

The total partial wave cross sections are shown in Fig. 4. The destructive interference between the $S_{11}(1535)$ and $S_{11}(1650)$ leads to the dip in the total S_{11}-partial wave cross section around $W = 1.64$ GeV (dotted line). The effect from the $P_{11}(1710)$ state is shown by the dashed line, Fig. 4. The contributions from other partial waves are found to be small. We also corroborate our previous results [63] where only minor contributions from spin $J \geqslant \frac{3}{2}$ resonance states were obtained. Both t-channel a_0 and ρ meson exchange and u-channel graphs give small effects. The inclusion of the higher spin state $D_{13}(1520)$ into the calculations is still important to reproduce the correct shape of the cross section. This feature is also found in many other calculations, e.g., [39,49]. It is interesting to note that importance of the $P_{11}(1710)$ resonance contribution has recently been found in [48] which is in line with our previous results [14,40].

Since the main contributions in our calculations come mainly from the S_{11} and P_{11} partial waves it is interesting

to trace back the interference effect between them. Neglecting the higher partial waves the differential cross section can be written in the form

$$\frac{d\sigma}{d\cos(\theta)} \sim 1 + \alpha \, \sin^2\left(\frac{\theta}{2}\right), \qquad (8)$$

where θ is a scattering angle and $\alpha = \left(\frac{|S_{11}-P_{11}|^2}{|S_{11}+P_{11}|^2} - 1\right)$ only depends on the c.m. energy. Then the angular distribution should have a maximum (minimum) at forward angles depending on the relative phase between the nonvanishing S_{11} and P_{11} amplitudes. In our calculation the interference between S_{11} and P_{11} partial waves produces a peak at forward scattering angles and energies above $W = 1.67$ GeV, see Fig. 3. As a result the signal from the $P_{11}(1710)$ resonance becomes more transparent for forward scattering. This is in line with the data of Richards *et al.* [3] confirming our guess about the production mechanism. The inclusion of higher partial waves would modify Eq. (8). However these contributions are relatively small (see Fig. 4) thus producing only minor deviations from the distribution Eq. (8).

Note, that due to numerous problems with the experimental data our calculations above $W = 1.6$ GeV are only partly constrained by experiment. Indeed, once the data [5,6] are neglected there are only 30 data points from experiment [3]. This data has relatively large error bars and seems not to be fully consistent with other measurements [7]. Therefore, the results for the differential cross section might be regarded as a prediction rather than an outcome of the fit. This demonstrates an urgent need for new measurements of the $\pi^- N \to \eta N$ reactions above $W = 1.6$ GeV. This would be a challenge for the the upcoming pion-beams experiment carried out by the HADES collaboration at GSI.

FIG. 4. (Color online) Total partial wave cross section $\pi^- p \to \eta n$ vs. experimental data.
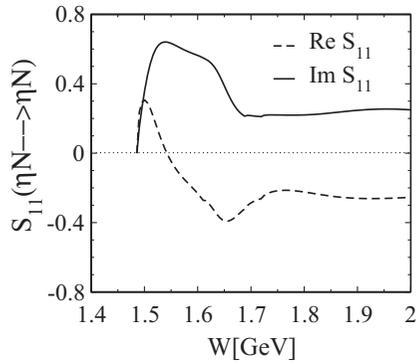
FIG. 5. Calculated S_{11} partial wave amplitude of the elastic ηN scattering.

B. $\eta N \rightarrow \eta N$ amplitude and ηN scattering lengths

The result for the $\eta N \rightarrow \eta N$ transition amplitude in the S_{11} partial wave is presented in Fig. 5. Close to threshold the elastic ηN scattering is completely determined by the contribution of the $S_{11}(1535)$ resonance. At higher energies the excitation of $S_{11}(1650)$ also becomes important. The interference between those two S_{11} states produces an excess structure in the imaginary part of the amplitude at $W = 1.65$ GeV.

The rapid variation of the S_{11} amplitude close to threshold indicates that this energy dependence should be taken into account when the ηN scattering length is calculated. Here we use the definition for the effective range expansion from [87]

$$\frac{q_{\text{c.m.}}}{S_{11}^{\eta N}} + i q_{\text{c.m.}} = \frac{1}{a_{\eta N}} + \frac{r_0}{2} q_{\text{c.m.}}^2 + s \, q_{\text{c.m.}}^4, \quad (9)$$

where $S_{11}^{\eta N}$ is an elastic partial S-wave amplitude, and $a_{\eta N}$, r_0 and s are scattering length, effective range, and effective volume, respectively. The results are shown in Table VI in comparison with values deduced from other coupled-channel calculations (results published before 1997 are discussed in [87]). The obtained value of $a_{\eta N}$ is very close to our previous results [39]. The values for the real part deduced in [88] and [87] are lower than in this work. The study [88] gives 1.550 GeV for the mass and 204 MeV for the width of the $S_{11}(1535)$ state which are somewhat greater than in the present calculation. This could be one of the reasons for the differences in Re $a_{\eta N}$.

In [87] only the $S_{11}(1535)$ state is taken into account to calculate transition amplitudes to the ηN channel. Since the parameters of $S_{11}(1535)$ in [87] are close to the values obtained in the present study the observed difference in

Re $a_{\eta N}$ might be attributed to the different treatment of background contributions which have been assumed in [87] to be energy-independent. The second piece of uncertainty is related to the quality of the world data of $\pi N \rightarrow \eta N$ scattering. Hence, precise measurements of this reaction would provide an additional constraint on ηN scattering length.

The nonvanishing imaginary part of $a_{\eta N}$ is mostly driven by rescattering in the πN channel. Since the largest contributions to the scattering length are produced by the $S_{11}(1535)$ state the imaginary part of $a_{\eta N}$ is strongly influenced by the decay branching ratio of this resonance to πN. Only a minor effect is found from the rescattering induced by background contributions and inelastic flux to the $2\pi N$ channel. Since the $\pi N N^*(1535)$ coupling is well fixed an agreement in Im($a_{\eta N}$) between various model calculations can be expected provided that unitarity is maintained.

The obtained value of the scattering length should be taken with care when in-medium properties of the η meson are considered. As it has already been pointed out in [87] the S_{11} amplitude has a strong energy dependence—a feature which might affect the η potential. The second reason is that properties of the $S_{11}(1535)$ resonance might also be subjected to in-medium modifications [89]. Both effects should be taken into account when η-meson properties in nuclei are studied.

C. $\gamma N \rightarrow \eta N$ below 1.89 GeV

The results of our calculation of the differential cross section in comparison with the recent Crystal Ball/MAMI measurements are shown in Fig. 6. Our calculations demonstrate a nice agreement with the experimental data in the whole kinematical region. The first peak is related to the $S_{11}(1535)$ resonance contribution. Similar to the $\pi^- p \rightarrow \eta n$ reaction the $S_{11}(1650)$ and $S_{11}(1650)$ states interfere destructively producing a dip around $W = 1.68$ GeV. Though the effect from the $P_{11}(1710)$ state is only minor, the contribution from this resonance produces a rapid change in the M_{1-} photoproduction multipole, see Sec. IV E. The coherent sum of all partial waves leads to the more pronounced effect from the dip at forward angles. Note that the resonance contribution to the photoproduction reaction stems from two sources: the first is related to the direct electromagnetic excitation of the nucleon resonance and the second comes from rescattering, e.g., $\gamma p \rightarrow \pi N \rightarrow \eta N$, Eq. (4). At this stage the hadronic transition amplitudes, e.g., $T_{\pi N \rightarrow \eta N}$ become an important part of the production mechanism. The sum of these contributions in the P_{11} wave turns out to be destructive which reduces the overall contribution from the $P_{11}(1710)$ state. We also

TABLE VI. Calculated scattering length and effective range in comparison with results from other works.

Reference	$a_{\eta N}$(fm)	r_0(fm)
present work	$0.99 \pm 0.08 + i 0.25 \pm 0.06$	$-1.98 \pm 0.1 - i 0.43 \pm 0.15$
[39]	$0.99 + i 0.34$	$-2.08 - i 0.81$
[88]	$0.734 \pm 0.026 + i 0.269 \pm 0.019$	
[87]	$0.75 \pm 0.04 + i 0.27 \pm 0.03$	$-1.5 \pm 0.13 - i 0.24 \pm 0.04$
[90]	$0.43 + i 0.21$	
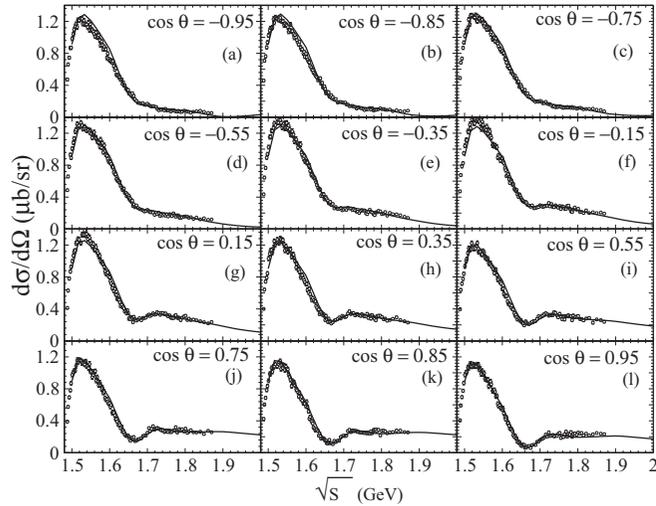
FIG. 6. Differential ηp cross section vs. recent MAMI data [35].

FIG. 8. (Color online) $\gamma p \to \eta p$ partial wave cross sections vs. measurements [20,21,38].

corroborate our previous findings [14] where a small effect from the ωN threshold was found. We also do not find any strong indication for contributions from a hypothetic narrow P_{11} state with a width of 15–20 MeV around $W = 1.68$ GeV. It is natural to assume that the contribution from this state would induce a strong modification of the beam asymmetry for energies close to the mass of this state. This is because the beam asymmetry is less sensitive to the absolute magnitude of the various partial wave contributions but strongly affected by the relative phases between different partial waves. Thus even a small admixture of a contribution from a narrow state might result into a strong modification of the beam asymmetry in the energy region of $W = 1.68$ GeV.

In Fig. 7 we show the calculation of the photon-beam asymmetry in comparison with the GRAAL measurements [22]. One can see that even close to the ηN threshold where our calculations exhibit a dominant S_{11} production mechanism (see Fig. 8) the beam asymmetry is nonvanishing for angles $\cos(\theta) \geqslant -0.2$. This shows that this observable is

very sensitive to very small contributions from higher partial waves. At $W = 1.68$ GeV and forward angles the GRAAL measurements show a rapid change of the asymmetry behavior. We explain this effect by a destructive interference between the $S_{11}(1535)$ and $S_{11}(1650)$ resonances which induces the dip at $W = 1.68$ GeV in the S_{11} partial wave. The strong drop in the S_{11} partial wave modifies the interference between S_{11} and other partial waves and changes the asymmetry behavior. Note that the interference between $S_{11}(1535)$ and $S_{11}(1650)$ and the interference between different partial waves are of different nature. The overlapping of the $S_{11}(1535)$ and $S_{11}(1650)$ resonances does not simply mean a coherent sum of two independent contributions, but also includes rescattering (coupled-channel effects). Such interplay is hard to simulate by the simple sum of two Breit-Wigner forms since it does not take into account rescattering due to the coupled-channel treatment.

The GRAAL collaboration finds no evidence for a narrow state around $W = 1.68$ GeV. We also find no strong need for the narrow P_{11} resonance contribution to describe the asymmetry data. Taking contributions from the established states into account our results are in close agreement with the experimental data [22].

D. $\gamma N \to \eta N$ above 1.89 GeV

Since the MAMI measurements are available up to $W = 1.89$ GeV the calculations in the region $W = 1.89, \ldots, 2.0$ GeV are constrained by the combined data set constructed out of the recent CLAS and CB-ELSA/TAPS [20,43] data. Due to some inconsistencies between these two experiments [41,42] we did not try to fit the data above $W = 2.0$ GeV but instead extrapolate our calculation into the higher energies. In this region the t-channel exchange starts to play a dominant role. One of the accepted prescriptions is to use a Reggeized t-channel meson exchange as suggested in [24]. We do not follow this procedure here but include all t-channel exchanges into the interaction kernel. This allows for a consistent unitary treatment of resonance and background contributions. The calculated differential cross section is presented in Fig. 9 as a function of the scattering angle. Except for the energy bin $W = 2.097$ GeV our results are found to be in close agreement with the CLAS measurements. The major

FIG. 7. Calculated beam asymmetry. Experimental data are taken from [22] (GRAAL07).
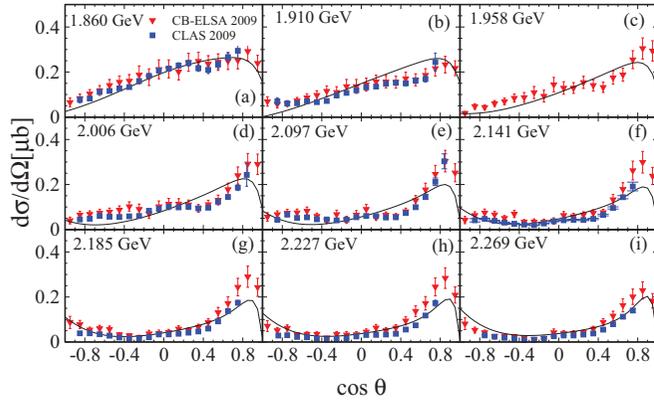
FIG. 9. (Color online) Differential ηp cross section as a function of the scattering angle. The data are taken from CLAS 2009 [43] and CB-ELSA [20].

contribution to the differential cross section at forward angles comes from ρ- and ω-meson exchanges. The effect from the ϕ meson is small due to the weakness of the ϕNN coupling as dictated by the OZI rule [91–93]. We also checked for the contributions from the Primakoff effect which is found to be negligible at these energies.

It is interesting to compare our calculations with the data [20,43] at forward angles plotted as a function of the c.m. energy, see Fig. 10. The cusp due to the ωN production threshold is clearly seen in our calculations around $W = 1.72$ GeV. The quality of the data is still not good enough to unambiguously resolve the cusp induced by the ωN threshold in the experimental data. Note, that the calculations are done assuming a stable ω meson. Taking into account the final ω width would smear out this effect. Since the ωN threshold lies 45 MeV above the dip position ($W = 1.68$ GeV) we conclude that this effect cannot explain the dip in the differential cross section. This conclusion is opposite to that drawn in [27].

The discrepancy between the CLAS [43] and CB-ELSA/TAPS data is better seen at $\cos(\theta) = 0.75$ whereas for $\cos(\theta) = 0.85$ the measurements are found to be in better agreement. One of the interesting features observed in the recent CB-ELSA data is a sudden rise of the differential cross section at $W = 1.92$ GeV. The effect is more pronounced at $\cos(\theta) = 0.85, \ldots, 0.95$ and is absent at other scattering angles. This phenomena might be attributed to sidefeeding
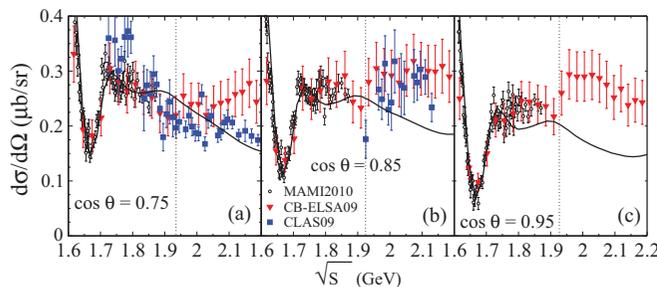
FIG. 10. (Color online) Differential ηp cross section as a function of c.m. energy at fixed forward angles. Data are taken from CLAS 2009 [43], CB-ELSA [20], and MAMI2010 [35].
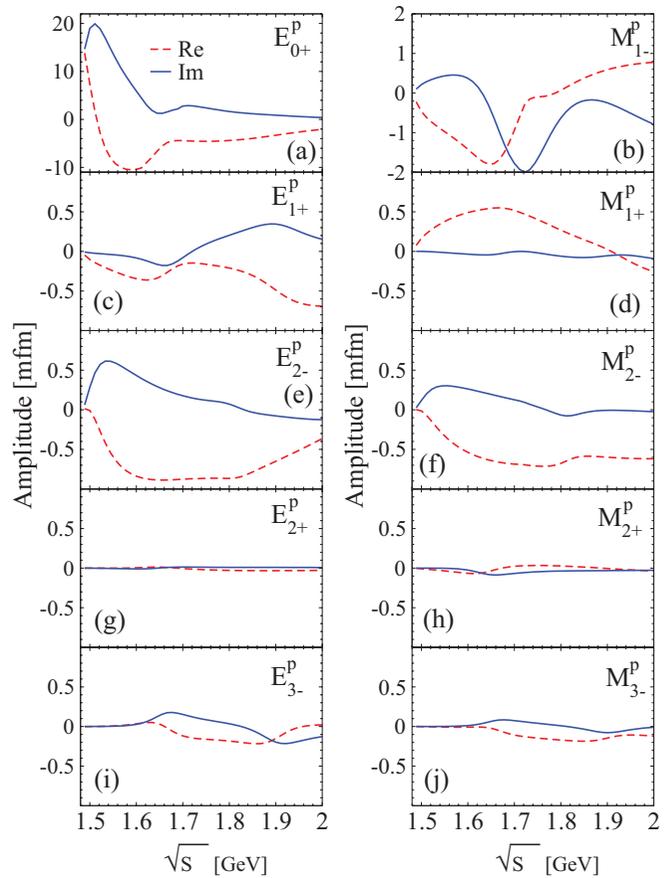
FIG. 11. (Color online) $\gamma p \to \eta p$ multipoles extracted in the present study.

from of one of the inelastic channels [e.g., ϕN, $a_0(980)N$, $f_0(980)$, or $\eta'N$]. However the problem with normalization inconsistencies between the CLAS and CB-ELSA data should be solved first before any physical interpretation can be given.

E. η-photoproduction multipoles

The extracted $\gamma p \to \eta p$ multipoles are presented in Fig. 11. The major contribution to the E_{0+} multipole comes from the $S_{11}(1535)$ resonance. The second $S_{11}(1650)$ plays an important role in the region $W = 1.6, \ldots, 1.7$ GeV. We corroborate our previous results [14] where only a small effect from the spin-$\frac{5}{2}$ states has been found. A very small signal from the $F_{15}(1680)$ resonance is seen in the E_{3-} and M_{3-} amplitudes at $W = 1.68$ GeV.

It is interesting to note that the effect of $D_{13}(1520)$ is clearly seen in the E_{2-} and M_{2-} though the overall contribution from this state turns out to be small. The M_{1-} multipole is affected by the Roper and $P_{11}(1710)$ resonances leading to the rapid change in both real and imaginary parts of the amplitude at $W = 1.7$ GeV. In the region $W = 1.48, \ldots, 1.6$ GeV both the imaginary and the real parts of all multipoles with $l \neq 0$ are of the order of magnitude smaller than E_{0+} due to the strong dominant contribution from $S_{11}(1535)$. However for higher energies the influence of amplitudes with $l \neq 0$ becomes also important.

V. CONCLUSION

We have performed a coupled-channel analysis of pion- and photon-induced reactions including the recent η-photoproduction data from the Crystal Ball/MAMI collaboration. In the region $W = 1.89, \ldots, 2.0$ GeV our solution is constrained by the combined data set built from the recent CLAS and CB-ELSA/TAPS measurements. The dip in the differential cross sections at $W = 1.68$ GeV reported in [35] is described in terms of an interference of the $S_{11}(1535)$ and $S_{11}(1650)$ states. We stress that such an interference also includes coupled-channel effects and rescattering which is hard to simulate by a simple sum of two Breit-Wigner contributions. The additional contribution at $W = 1.68$ GeV comes from the M_{1-} multipole where the excitation of the $P_{11}(1710)$ leads to a rapid change of the real and imaginary parts of the amplitude. We conclude that the cusp due to the ωN threshold seen at 1.72 GeV is not important for the explanation of the dip at $W = 1.68$ GeV. However the quality of the data is still not sufficient to resolve the threshold effect completely.

Above $W = 1.9$ GeV the t-channel ρ and ω exchanges start to play a dominant role in the calculations. The effect from the ϕ-meson exchange is less important because of the smallness of the ϕNN coupling. We have also checked for the contribution from the Primakoff-effect which is found to be negligible. In the region $W = 1.9, \ldots, 2.2$ GeV our calculations tend to be in closer agreement with the CLAS data.

It is interesting to note that above $W = 1.92$ GeV the cross sections of the CB-ELSA/TAPS collaboration indicate a sudden rise from 0.2 μb up to 0.3 μb. The effect is observed only for scattering angles $\cos(\theta) = 0.85, \ldots, 0.95$. This phenomenon might be attributed to sidefeeding from of one of the inelastic channels [e.g., ϕN, $a_0(980)N$, $f_0(980)$, or $\eta' N$]. However the origin of the normalization discrepancies between the CLAS and CB-ELSA/TAPS data should first be understood before any physical interpretation can be given.

In the $\pi^- p \to \eta n$ reaction the main effect comes from three resonances $S_{11}(1535)$, $S_{11}(1650)$, and $P_{11}(1710)$. Similar to η photoproduction on the proton the overlap of the $S_{11}(1535)$ and $S_{11}(1650)$ states produces a dip around $W = 1.68$ GeV. For energies $W > 1.68$ GeV the contribution from $P_{11}(1710)$ is found to be important. The above reaction mechanism for the $(\gamma/\pi)N \to \eta N$ reaction is in line with our early findings [14] where the resonance like-structure in η photoproduction at $W = 1.68$ GeV on the neutron was explained by the excitations of the $S_{11}(1650)$, and $P_{11}(1710)$ resonances.

We conclude that further progress in understanding of η-meson production would be hardly possible without new measurements of the $\pi N \to \eta N$ reaction. The experimental investigation of this reaction would help to establish the resonance contributions to the η photoproduction above $W > 1.6$ GeV. Finally, the study of the ηN channel with pion beams would solve the question whether the observed phenomena in η photoproduction have their counterparts in $\pi N \to \eta N$ scattering.

[1] I. Aznauryan *et al.*, arXiv:0907.1901 [nucl-th] (2009).

[2] W. Jones, D. Binnie, A. Duane, J. Horsey, and D. Mason, Phys. Lett. **23**, 597 (1966).

[3] W. Richards *et al.*, Phys. Rev. D **1**, 10 (1970).

[4] F. Bulos *et al.*, Phys. Rev. **187**, 1827 (1969).

[5] R. M. Brown *et al.*, Nucl. Phys. B **153**, 89 (1979).

[6] R. Baker *et al.*, Nucl. Phys. B **156**, 93 (1979).

[7] M. Clajus and B. Nefkens, πN Newslett. **7**, 76 (1992).

[8] V. Kuznetsov *et al.*, arXiv:hep-ex/0601002 (2006).

[9] V. Kuznetsov, S. Churikova, G. Gervino, F. Ghio, B. Girolami, D. Ivanov, J. Jang, A. Kim, W. Kim, A. Ni, Yu. Vorobiev, M. Yurov, and A. Zabrodin, Phys. Lett. B **647**, 23 (2007).

[10] I. Jaegle *et al.* (CBELSA/TAPS Collaboration), Phys. Rev. Lett. **100**, 252002 (2008).

[11] I. Jaegle *et al.*, Eur. Phys. J. A **47**, 89 (2011).

[12] Y. I. Azimov, V. Kuznetsov, M. Polyakov, and I. Strakovsky, Eur. Phys. J. A **25**, 325 (2005).

[13] D. Diakonov, V. Petrov, and M. V. Polyakov, Z. Phys. A **359**, 305 (1997).

[14] V. Shklyar, H. Lenske, and U. Mosel, Phys. Lett. B **650**, 172 (2007).

[15] A. Anisovich *et al.*, Eur. Phys. J. A **41**, 13 (2009).

[16] M. Döring and K. Nakayama, Phys. Lett. B **683**, 145 (2010).

[17] V. E. Tarasov, W. J. Briscoe, H. Gao, A. E. Kudryavtsev, and I. I. Strakovsky, Phys. Rev. C **84**, 035203 (2011).

[18] A. Martinez Torres and E. Oset, Phys. Rev. Lett. **105**, 092001 (2010).

[19] M. Dugger *et al.* (CLAS Collaboration), Phys. Rev. Lett. **89**, 222002 (2002).

[20] V. Crede *et al.* (CBELSA/TAPS Collaboration), Phys. Rev. C **80**, 055202 (2009).

[21] O. Bartholomy *et al.* (CB-ELSA Collaboration), Eur. Phys. J. A **33**, 133 (2007).

[22] O. Bartalini *et al.* (GRAAL Collaboration), Eur. Phys. J. A **33**, 169 (2007).

[23] X.-H. Zhong and Q. Zhao, Phys. Rev. C **84**, 045207 (2011).

[24] W.-T. Chiang, S. N. Yang, L. Tiator, M. Vanderhaeghen, and D. Drechsel, Phys. Rev. C **68**, 045202 (2003).

[25] T. Feuster and U. Mosel, Phys. Rev. C **59**, 460 (1999).

[26] C. S. An and B. Saghai, Phys. Rev. C **84**, 045204 (2011).

[27] A. Anisovich *et al.*, arXiv:1108.3010 [hep-ph] (2011).

[28] R. Shyam and O. Scholten, Phys. Rev. C **78**, 065201 (2008).

[29] K. Nakayama, Y. Oh, and H. Haberzettl, J. Korean Phys. Soc. **59**, 224 (2011).

[30] K.-S. Choi, S.-i. Nam, A. Hosaka, and H.-C. Kim, J. Phys. G **36**, 015008 (2009).

[31] X.-H. Zhong, Q. Zhao, J. He, and B. Saghai, Phys. Rev. C **76**, 065205 (2007).

[32] A. Fix, L. Tiator, and M. Polyakov, Eur. Phys. J. A **32**, 311 (2007).

[33] A. M. Gasparyan, J. Haidenbauer, C. Hanhart, and J. Speth, Phys. Rev. C **68**, 045207 (2003).

[34] D. Ruic, M. Mai, and U.-G. Meissner, Phys. Lett. B **704**, 659 (2011).

[35] E. F. McNicoll *et al.* (Crystal Ball collaboration at MAMI), Phys. Rev. C **82**, 035208 (2010).
[36] R. A. Arndt, Y. I. Azimov, M. V. Polyakov, I. I. Strakovsky, and R. L. Workman, Phys. Rev. C **69**, 035208 (2004).
[37] Y. I. Azimov, R. Arndt, I. Strakovsky, R. Workman, and K. Goeke, Eur. Phys. J. A **26**, 79 (2005).
[38] V. Crede *et al.* (CB-ELSA Collaboration), Phys. Rev. Lett. **94**, 012004 (2005).
[39] G. Penner and U. Mosel, Phys. Rev. C **66**, 055211 (2002).
[40] G. Penner and U. Mosel, Phys. Rev. C **66**, 055212 (2002).
[41] A. Sibirtsev, J. Haidenbauer, S. Krewald, and U.-G. Meissner, Eur. Phys. J. A **46**, 359 (2010).
[42] B. Dey and C. A. Meyer, arXiv:1106.0479 [hep-ph] (2011).
[43] M. Williams *et al.* (CLAS Collaboration), Phys. Rev. C **80**, 045213 (2009).
[44] S. Prakhov *et al.* (Crystal Ball Collaboration), Phys. Rev. C **72**, 015203 (2005).
[45] J. S. Danburg *et al.*, Phys. Rev. D **2**, 2564 (1970).
[46] N. C. Debenham *et al.*, Phys. Rev. D **12**, 2545 (1975).
[47] W. Deinet *et al.*, Nucl. Phys. B **11**, 495 (1969).
[48] M. Shrestha and D. M. Manley, Phys. Rev. C **86**, 045204 (2012).
[49] M. Batinic, I. Slaus, A. Svarc, and B. M. K. Nefkens, Phys. Rev. C **51**, 2310 (1995); **57**, 1004 (1998).
[50] F. Renard *et al.* (GRAAL Collaboration), Phys. Lett. B **528**, 215 (2002).
[51] B. Krusche *et al.*, Phys. Rev. Lett. **74**, 3736 (1995).
[52] T. Nakabayashi *et al.*, Phys. Rev. C **74**, 035202 (2006).
[53] D. Elsner *et al.* (CBELSA/TAPS Collaboration), Eur. Phys. J. A **33**, 147 (2007).
[54] A. Bock *et al.*, Phys. Rev. Lett. **81**, 534 (1998).
[55] J. Ajaka *et al.*, Phys. Rev. Lett. **81**, 1797 (1998).
[56] L. Tiator, D. Drechsel, G. Knöchlein, and C. Bennhold, Phys. Rev. C **60**, 035210 (1999).
[57] J. Hartmann (CBESLA/TAPS Collaboration), AIP Conf. Proc. **1432**, 279 (2012).
[58] R. L. Workman, W. J. Briscoe, M. W. Paris, and I. I. Strakovsky, Phys. Rev. C **85**, 025201 (2012).
[59] R. A. Arndt, W. J. Briscoe, I. I. Strakovsky, and R. L. Workman, Phys. Rev. C **74**, 045205 (2006).
[60] R. Arndt, W. Briscoe, I. Strakovsky, and R. Workman, Eur. Phys. J. A **35**, 311 (2008).
[61] T. Feuster and U. Mosel, Phys. Rev. C **58**, 457 (1998).
[62] D. M. Manley, R. A. Arndt, Y. Goradia, and V. L. Teplitz, Phys. Rev. D **30**, 904 (1984).
[63] V. Shklyar, G. Penner, and U. Mosel, Eur. Phys. J. A **21**, 445 (2004).
[64] V. Shklyar, H. Lenske, and U. Mosel, Phys. Rev. C **72**, 015210 (2005).
[65] B. C. Pearce and B. K. Jennings, Nucl. Phys. A **528**, 655 (1991).
[66] P. F. A. Goudsmit, H. J. Leisi, E. Matsinos, B. L. Birbrair, and A. B. Gridnev, Nucl. Phys. A **575**, 673 (1994).
[67] E. Oset and A. Ramos, Nucl. Phys. A **635**, 99 (1998).
[68] V. Shklyar, H. Lenske, U. Mosel, and G. Penner, Phys. Rev. C **71**, 055206 (2005).
[69] J. Beringer *et al.* (Particle Data Group), Phys. Rev. D **86**, 010001 (2012).
[70] R. M. Davidson and R. Workman, Phys. Rev. C **63**, 025210 (2001).
[71] T. P. Vrana, S. A. Dytman, and T. S. H. Lee, Phys. Rep. **328**, 181 (2000).
[72] R. E. Cutkosky and S. Wang, Phys. Rev. D **42**, 235 (1990).
[73] R. A. Arndt, Z.-J. Li, L. D. Roper, R. L. Workman, and J. M. Ford, Phys. Rev. D **43**, 2131 (1991).
[74] R. A. Arndt, I. I. Strakovsky, and R. L. Workman, Phys. Rev. C **53**, 430 (1996).
[75] V. Shklyar, H. Lenske, and U. Mosel (in preparation).
[76] L. Tiator, S. S. Kamalov, S. Ceci, G. Y. Chen, D. Drechsel, A. Svarc and S. N. Yang Phys. Rev. C **82**, 055203 (2010).
[77] M. Batinic, S. Ceci, A. Svarc, and B. Zauner, Phys. Rev. C **82**, 038203 (2010).
[78] A. Anisovich *et al.*, Eur. Phys. J. A **48**, 15 (2012).
[79] G. Hoehler, πN Newslett. **9**, 1 (1993).
[80] R. E. Cutkosky and S. Wang, Phys. Rev. D **42**, 235 (1990).
[81] R. E. Cutkosky, C. P. Forsyth, R. E. Hendrick, and R. L. Kelly, Phys. Rev. D **20**, 2839 (1979).
[82] M. Doring, C. Hanhart, F. Huang, S. Krewald, and U.-G. Meissner, Nucl. Phys. A **829**, 170 (2009).
[83] S. Ceci, A. Svarc, and B. Zauner, Phys. Rev. Lett. **97**, 062002 (2006).
[84] S. Ceci, A. Svarc, and B. Zauner, Few-Body Syst. **39**, 27 (2006).
[85] L. De Cruz, J. Ryckebusch, T. Vrancx, and P. Vancraeyveld, Phys. Rev. C **86**, 015212 (2012).
[86] T. W. Morrison, Ph.D. thesis, George Washington University, UMI-99-55477, 2000 (2000).
[87] A. M. Green and S. Wycech, Phys. Rev. C **55**, R2167 (1997).
[88] M. Batinic *et al.*, Phys. Scr. **58**, 15 (1998).
[89] J. Lehr, M. Post, and U. Mosel, Phys. Rev. C **68**, 044601 (2003).
[90] M. F. M. Lutz, G. Wolf, and B. Friman, Nucl. Phys. A **706**, 431 (2002).
[91] S. Okubo, Phys. Lett. **5**, 165 (1963).
[92] G. Zweig (1964), in *Developments in the Quark Theory of Hadrons*, Vol. 1, edited by D. Lichtenberg and S. Rosen (Hadronic Press, Nonantum, MA, 1980), pp. 22–101.
[93] J. Iizuka, Prog. Theor. Phys. Suppl. **37**, 21 (1966).